# RSC Advances

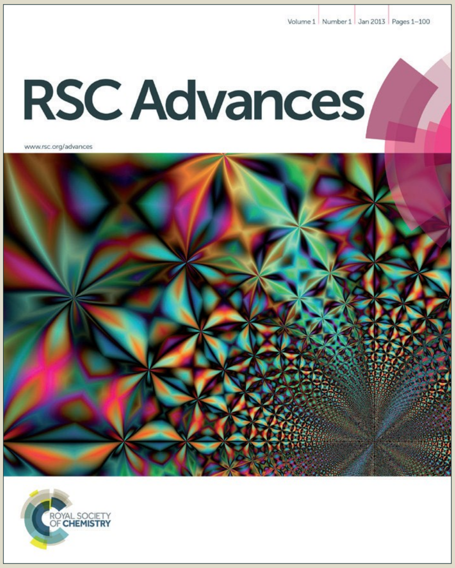

ROYAL SOCIETY OF CHEMISTRY

www.rsc.org/advances

# The One-step Oxidation of Methanol to Dimethoxymethane over Sulfated vanadia-titania Catalysts: Influence of Calcination Temperature

*Heqin Guo[a], Debao Li[a], Congbiao Chen[a], Litao Jia[a], Bo Hou[a]**

*[a] State Key Laboratory of Coal Conversion, Institute of Coal Chemistry, Chinese Academy of Sciences, Taiyuan, 030001, China.*

**Corresponding author: Tel. /Fax: +86 351 4040087. E-mail addresses:* houbo@sxicc.ac.cn,

**Abstract:**

The sulfated vanadia-titania catalysts were prepared by the rapid combustion method and calcined at different temperature, respectively. The influence of calcination temperature on the physicochemical properties of the catalysts was characterized by nitrogen adsorption( BET), X-ray diffraction(XRD), Fourier transform infrared spectroscopy (FTIR), inductively coupled plasma-optic emission spectroscopy (ICP-OES) , X-ray photoelectron spectroscopy(XPS), temperature-programmed reduction ($H_2$-TPR-MS), thermogravimetry(TG) and temperature programmed desorption of ammonia ($NH_3$-TPD) techniques. The catalytic activities were evaluated by the partial oxidation of methanol to dimethoxymethane (DMM). The results showed that the vanadia and sulfate were highly dispersed as the catalysts were calcined at 723 and 773 K. The reducibility of the highly dispersed vanndia was stronger than the aggregated vanadia. And the larger number of acidic sites was related to the higher dispersion of sulfate. Moreover, the higher dispersion of vanadia contributed to higher methanol conversion, and the stronger reducibility combined with larger number of acidic sites led to high

DMM selectivity. As a result, the catalysts calcined at 723 and 773 K presented higher methanol conversion and DMM selectivity than those calcined at 673 K or above 823 K.

**Keywords:** Sulfated vanadia-titania catalysts; Calcination Temperature; Methanol partial oxidation; Dimethoxymethane

## 1. Introduction

Dimethoxymethane ($CH_3OCH_2OCH_3$, DMM), as an important green down stream products of methanol, is widely used as diesel additive and building block in organic synthesis. There are numerous reports that DMM can be synthesized by the one-stage oxidation of methanol ($3CH_3OH + 1/2O_2 = CH_3OCH_2OCH_3 + 2H_2O$) [1–10]. In these cases, two types of active sites, including redox sites and acidic sites, were required for DMM synthesis. Here, the redox sites with active lattice oxygen atoms were considered to be involved in the initial formation of formaldehyde (FA) from $CH_3OH$, whereas acidic sites could catalyze the desired acetalization reactions of FA and $CH_3OH$ to DMM. Moreover, the acidic sites were also favorable to dimethyl ether (DME) formation, and the redox sites can catalyze methanol to FA/methyl formate (MF). Therefore, exact matching/cooperation of the redox properties and acidity is critical in getting high DMM selectivity.

Several catalysts, such as heteropoly acids[1-2], $SbRe_2O_6$[3], supported rhenium oxide[4], $Mo_{12}V_3W_{1.2}Cu_{1.2}Sb_{0.5}O_x$[9], Cu-ZSM-5[11], FeMo[12] and sulfated vanadia–titania[13-16], have been applied in DMM synthesis. Among the reported catalysts, the sulfated vanadia-titania catalysts (VTS) have been considered to be promising for DMM synthesis with high DMM selectivity at lower reaction temperature [13-14]. While, the physicochemical characteristics of this catalyst, especially the acidic and redox properties, are strongly related to the existing state of vanadia, sulfate and titania [14, 17-19]. Generally, the high dispersion of vanadia and sulfate contributes to stronger reducibility and more acidic sites. Moreover, the anatase $TiO_2$ is usually more active than rutile $TiO_2$, due to the fact that the properties of the vanadium species present on the surface of the anatase phase have different acid-basic and redox properties, while those present on the surface of the rutile polymorph phase resemble the properties of those of pure $V_2O_5$[20]. Therefore, to obtain the best catalytic performance of VTS catalyst in methanol oxidation reaction, it is necessary to optimize the existing of the vanadia, titania and sulfate. A reasonable and simple approach towards the solution of this problem is related with the optimization of calcination temperature. Although several attempts have been made to improve the catalytic performance of vanadia-titania catalysts by optimizing the calcination temperature [21-23], those for the sulfated vanadia-titania catalysts have received little attention.

In the present study, the VTS catalysts were prepared by the rapid combustion method and calcined at different temperature. The influence of calcination temperature on the physico-chemical properties of catalysts were studied by XRD, FTIR, BET, ICP-OES, XPS, TG , $H_2$-TPR-MS and $NH_3$-TPD techniques. Moreover, the samples were also tested in the methanol partial oxidation reaction. The aim of this work was to obtain matched redox and acidity to optimize DMM selectivity.

## 2. Experimental

**Catalyst preparation:** The VTS catalysts were prepared by the rapid combustion (RC) method. In the typical synthesis: 13.89 ml $TiCl_4$ was added to 37.86 ml 67 wt% $HNO_3$ under vigorously stirring under $N_2$ atmospheres, and then 6.22 g $NH_4VO_3$, 3.37 g Ti $(SO_4)_2$ and 73.7

g carbamide were added to the solution, the obtained mixture was stirred until the $NH_4VO_3$ and carbamide were completely dissolved, and then calcined under 673, 723, 773, 823 and 873 K, respectively, for 15 min. The obtained catalysts were marked as VTS-673, VTS-723, VTS-773, VTS-823 and VTS-873, respectively. For comparison, the sulfated vanadia-titania sample without calcination and the pure rutile $TiO_2$ calcined at 973 K was prepared by the same method, which were marked as VTS and $TiO_2$-R, respectively.

**2.2 Catalyst characterization**

The specific surface areas of the catalysts were measured by the BET method with a Micromeritics model ASAP 2000 using nitrogen at −196℃. Prior to measurements, all catalysts were outgassed at 150℃ under $1 \times 10^{-5}$ Torr residual pressure. XRD patterns were measured on a Bruker Advanced X-Ray Solutions/D8-Advance using Cu Kα radiation (λ = 1.5404Å). The skeletal FT-IR spectra were recorded with a Bruker Vector 22 FTIR spectrophotometer (DTGS detector) operating in the 4000–400 $cm^{-1}$ range, with a resolution of 2 $cm^{-1}$ and100 acquisition scans. In each experiment, 2 mg of sample were mixed with 198 mg of KBr. A spectrum was recorded at room temperature. TG was carried out on a SetaramTGA-92 analyzer with a heating speed of 10 K/min in the 303–1073 K range under air in a flow of 50 ml/min. The elemental analysis (Ti, V, and S) was performed by inductively coupled plasma-opticemission spectroscopy (ICP-OES). The XPS measurements were performed in a Physical Electronics Company Quantum-2000 Scaning ESCA Microprobe equipped with a Al X-ray source (23.3 mA and 1.5 kV), a solid angle acceptance lens and a hemispherical electron analyzer. Samples were compressed in small cup under the pressure of 5 kg/cm2 for 30 s and supported on a holding ceramic carousel. The positive charge, developed on the samples due to the photoejection process was compensated by a charge neutralizer (Low energy electron and Low energy ion beam). The residual pressure in the spectrometer chamber was 5×10-7 Pa during data acquisition. The analyzed area of the sample was100 um and the Energy region of the photoelectrons were scanned at a pass energy of 29.35 eV. The resolution was 0.68 eV. The binding energies of O 1s, V 2p, Ti 2p and S 2p were referenced to the C 1s band at 284.8 eV. The data was treated on Phi Multipack Program, Gaussian/Lorentzian =80%. Atomic concentration ratios were calculated by correcting the measured intensity ratios with the manufacturer supplied sensitivity factor. The $H_2$-TPR-MS was carried in continuous mode using a U-type quartz micro-reactor (3.5 mm in diameter). A sample of about 25 mg was contacted with a $H_2$: Ar mixture (5% $H_2$/Ar) at a total flow rate of 60 $cm^3$/min. The inlet and outlet gas compositions were measured using a quadrupole mass spectrometer QMC 311 Balzers. The $NH_3$-TPD spectra were recorded in a fixed-bed reactor system equipped with a gas chromatograph. The catalyst (200 mg) was pretreated at 773 K under Ar flow (60 ml / min) for 2 h and then cooled to 373 K. Then $NH_3$ was introduced into the flow system. The TPD spectra were recorded at a temperature rising rate of 10 K/min from 373 to 900 K.

**Catalyst test** The catalytic oxidation reaction was carried out in a continuous flow fixed–bed reactor containing catalyst (1.0 g) diluted with ground quartz. Before reaction, catalysts were treated in flowing 10% $O_2$/Ar (85 $cm^3$/min) for 2 h at 673 K. And then the methanol was introduced into the reaction zone by bubbling $O_2$/Ar (1/9) through a glass saturator filled with methanol (99.9%) maintained at 278 K. The feed composition was maintained as Ar: $O_2$: $CH_3OH$=84.6:9.4:6.0 (v/v/v). The reaction products were analyzed by on-line gas chromatography (GC-950) using a Propack T column and a TDX-01 column connected to TCD detector and FID detector, respectively. The gas lines were kept at 373 K to prevent condensation of the reactant and products. The reaction was carried out at atmospheric pressure. The product selectivity was calculated on carbon molar base: Si = Yini/∑Yini ×100%, where i is $CH_3OCH_2OCH_3$, $CH_3OCH_3$, HCHO, $HCOOCH_3$, $CO_x$, Si is the selectivity of product i, Yi is the number of carbon atom of product i, and ni is the molar of product i.

## 3. Results and Discussion

### 3.1 physico-chemical characterization

The textual properties of the catalysts are listed in Table 1. The surface area of the catalysts increases with increasing calcination temperature, and reached the maximum (120.19 $m^2.g^{-1}$) on VTS-773 sample. While, as the calcination temperature continued to increase, the surface area decreased, only 12.58 $m^2.g^{-1}$ on VTS-873 sample.

The XRD patterns of the catalysts are shown in Fig.1. On VTS-673 sample, no diffractions of titania was observed, indicating that the titania might exist as amorphous. While, the typical diffractions of anatase $TiO_2$($TiO_2$-A) was observed on VTS-723 and VTS-773 samples. On VTS-823 and VTS-873 samples, the $TiO_2$-A and rutile $TiO_2$ ($TiO_2$-R) were coexisted. While, the intensities of $TiO_2$-R diffraction peaks were stronger on VTS-873 sample than VTS-823 sample [24]. This result indicated that the increasing temperature caused the transformation of $TiO_2$-A to $TiO_2$-R. Moreover, no diffraction peaks of crystalline $V_2O_5$ were observed as the calcination temperature was below 823K, implying that the vanadia was highly dispersed or the $V_2O_5$ crystalline was less than 4 nm [14]. The typical diffraction peaks of $V_2O_5$ crystalline [14, 25-26] appeared on VTS-873 sample, which indicated the aggregation of vanadia.

To further study the existing state of vanadia, the FTIR spectra were carried out (see Fig. 2). For VTS-673, VTS-723 and VTS-773 samples, a threshold around 1000 $cm^{-1}$ were detected , which could be assigned to the bands for polyvanadate species (V-O-V) bonded to the surface of $TiO_2$[14]. While, for VTS-823 and VTS-873 samples, a band at 1022 $cm^{-1}$ due to the microcrystalline $V_2O_5$ appeared, simultaneously with the decrease of the peak intensity at 1000 $cm^{-1}$, suggesting the formation of crystalline $V_2O_5$ [14-17, 25-26]. Combined with the XRD results, it can be deduced that the vanadia should be highly dispersed on VTS-673, VTS-723 and VTS-773 samples, while aggregated as crystalline $V_2O_5$ on VTS-823 and VTS-873 samples. In addition, a typical band at 1137 $cm^{-1}$ corresponding to $SO_4^{2-}$[27] was detected for all of the samples, which indicated that the S existed as sulfate. While, its intensity weakened with the increase of calcination temperature, implying the decrease of sulfate content.

Table 1 lists the binding energies (BE) as well as the surface and bulk composition from XPS and ICP-OES. The binding energies of Ti $3d_{5/2}$ for the catalysts were 458.2-458.6 eV, which suggested the presence of $Ti^{4+}$ [27-29]. The binding energies of $V2p_{3/2}$ for the catalysts were 517.1-516.4-517.2 eV, indicated the surface vanadia species were fully oxidized (oxidation state $V^{5+}$)[29]. The common peaks of O1s for both the catalysts were 529.6 and 532 eV, which belonged to the oxide oxygen and sulfate oxygen, respectively [27]. The binding energies at 168.7-169.5 eV (see Fig. 3.) was measured for $S2p_{3/2}$, which are typical of sulfur in the $S^{6+}$ oxidation state, as in $Na_2SO_4$ or $Fe_2(SO_4)_3$ [30].

The analysis of bulk and surface sulfate content showed that both the surface and bulk sulfate content decreased with the increase of calcination temperature, which might be due to the decomposition of sulfate (See TG result). Moreover, the surface sulfate content was higher than that of bulk, indicating that the sulfate mainly existed on the surface of the catalysts. Based on the surface area and the sulfate content, the number of S (atoms/nm$^2$) was calculated. The values for VTS-723 and VTS-773 were 3.38 and 2.74, respectively. While, those were 6.95, 4.20 and 14.54 for VTS-673, VTS-823 and VTS-873, respectively. According to the reported result [32], the necessary mole concentration of sulfate to form a monolayer was 3.9 S/nm$^2$. Thus, the sulfate was highly dispersed on VTS-723 and VTS-773 samples, while aggregated on VTS-673, VTS-823 and VTS-873 samples.

The $H_2$-TPR-MS was carried out to confirm the existing state of sulfate (in Fig. 4). Three types of product, $H_2O$, $SO_2$ and $H_2S$, were detected with their formation temperatures in parallel with the hydrogen consumption. According to the literature, the formation of $H_2O$ is due to the reduction of $VO_x$, while the $SO_2$ and $H_2S$ are due to the reduction of sulfate [32]. For VTS-673, VTS-823 and VTS-873, only $SO_2$ was detected (see Fig. 4 a, d and e). While, for VTS-723 and VTS-773 (see Fig. 4 b and c), both $H_2S$ and $SO_2$ were detected. It was reported [31-32] that the production of $SO_2$ and $H_2S$ during $H_2$ reduction was correspond to the reduction of bidentate sulfate species and the emission of only $SO_2$ was due to the reduction of pyrosulfate species. Combined with the present study, it was clear that the sulfate dispersed as bidentate sulfate on VTS-723 and VTS-773, while aggregated as pyrosulfate sulfate on other samples. In addition, the intensity of $SO_2$ on VTS-673 sample was stronger than those on VTS-823 and VTS-873 samples, which might be due to the decomposition of sulfate on VTS-823 and VTS-873 (see TG result).

To further study the reasons leading to the decreasing content of sulfate, the thermal stability of sulfate was characterized by TG on VTS sample (see Fig. 5.).The VTS sample exhibited four weight losing peaks at 379, 635, 768 and 884 K, respectively. The peak at 379 K is attributed to the removal of water, while those at 635, 768 and 884 K are corresponding to the decomposition of sulfate [31]. Combined with the above results, it can be deduced that the decreased content of sulfate was due to the decomposition of sulfate under high temperature.

**3.2 Redox and acidity properties**

In $H_2$-TPR process, the profiles of hydrogen consumption could reflect the redox property of metal oxide [31]. As shown in Fig. 4, for VTS-673, a major reducible peak was observed at 741 K, which shifted to 720 K on VTS-723 and VTS-773 samples, while shifted to 805 K on VTS-873. This result indicated that the catalysts calcined at 723 and 773 K exhibited stronger reducibility than those calcined at 673 K or above 823 K. The different reducibility of the catalysts could be due to the different existing state of vanadia. For VTS-723 and VTS-773 samples, the stronger reducibility was due to the high dispersion of vanadia. While, for VTS-823 and VTS-873 samples, the appearance of crystalline $V_2O_5$ led to poor reducibility.

The acidity of the catalysts was characterized by $NH_3$-TPD technique (see Fig. 6 and Table 2). All of the catalysts showed similar feature of $NH_3$ desorption, which spread in the temperature range of 400–700 K, indicating the acidity strength of the samples was similar.

However, the number of acidic sites among the catalysts was significantly different. For VTS-723 and VTS-773, the values were 745 and 817 μmol/g, which were much larger than those on VTS-673, VTS-823 and VTS-873. To quantitatively analyze the effect of the type of sulfate species on the number of acidic sites, the number of absorbed ammonia per sulfate species was calculated. The values were 1.18 and 1.50 for VTS-723 and VTS-773, and only 0.78, 0.79 and 0.89 for VTS-673, VTS-823 and VTS-873. As a result, the high dispersion of sulfate on VTS-723 and VTS-773 samples led to larger number of acidic sites, and the aggregation of sulfate on VTS-673, VTS-823 and VTS-873 samples resulted in small number of acidic sites.

### 3.3 Catalytic Performance

Fig. 7 shows the influence of calcination temperature on methanol conversion. As it can be seen, the VTS-723 and VTS-773 samples were more active than VTS-673, VTS-823 and VTS-873 samples. For example, at 403 K, the methanol conversion was only 19.51% on VTS-673 sample, while increased up to 43.53% and 42.72 % on VTS-723 and VTS-773, and then decreased to 0 % on VTS-873 sample. The catalytic performances at other temperatures were similar to 403 K. The previous reports [14, 17] showed that the catalytic activity of vanadia-based catalyst in methanol oxidation reaction is closely related to the existing state of vanadia. And the highly dispersed vanadia contributes to high activity, while the $V_2O_5$ crystalline exhibits low activity [33-36]. Combined with the XRD and FTIR results, it can be deduced that the high dispersion of vanadia on VTS-723 and VTS-773 contributed to high methanol conversion. On VTS-823 and VTS-873 samples, the appearance of crystalline $V_2O_5$ and the appearance of $TiO_2$-R led to the low methanol conversion.

Table 3 shows the effect of calcination temperature on DMM selectivity at similar methanol conversion (about 45%). The DMM selectivity showed similar changing trend to methanol conversion, and reached the maximum on VTS-723 and VTS-773 samples. That phenomenon could be explained by the difference of acidity and redox properties among these catalysts. According to the mechanism of the one-step synthesis of DMM from methanol reported by Liu [1], the methanol was primarily oxidized to FA on redox sites, and then the methanol reacted with FA to form DMM on acidic sites. Furthermore, our previous study [33-34] showed that the higher DMM selectivity on the vanadium-based catalysts was due to the stronger reducibility matched with larger number of the acidic sites. Combined with the present study, it can be deduced that the stronger reducibility of VTS-723 and VTS-773 could enhance the oxidation of methanol to FA, while the more number of acidic sites could enhance the acetalization reactions of FA and $CH_3OH$ to DMM and finally lead to high DMM selectivity. For catalysts calcined at 673 K or above 823 K, the poor reducibility and small number of acidic sites could not efficiently catalyze the first and the second reaction, leading to the low DMM.

## Conclusion

The calcination temperature has profound influence on catalyst structure, which in turn affected the acidity and reducibility as well as catalytic performance in the one-step oxidation of methanol to DMM. The highest dispersion of vanadia and sulfate was obtained on VTS-723 and VTS-773. The stronger reducibility and more acidic sites were closely related to highly dispersed vanadia and sulfate, while the poor reducibility and small acidic sites were relate to the aggregated vandia and sulfate. The highest activity and DMM selectivity obtained on VTS-723 and VTS-773 samples was due to the highest dispersion of vanadia and the corresponding stronger reducibility and large number of acidic sites.

## Acknowledgements

The authors gratefully acknowledge the Key Project of Natural Science Foundation of China (NO.21303241) and Key Project of Natural Science Foundation of Shanxi Province (NO. 2012021005-6).

## References

[1] H.C. Liu, E.S. Iglesia, J. Phys. Chem. B 2003, 107, 10840.

[2] H.C. Liu, E.S. Iglesia, J. Catal. 2004, 223, 161.

[3]Y.Z.Yuan, H.C.Liu, H.Imoto, T. Shido, Y.Iwasawa, J. Catal. 2000, 195, 51.

[4] Y.Z.Yuan, T. Shido, Y. Iwasawa, J. Phys. Chem. B 2002, 106, 4441.

[5] H.C. Liu, E.S. Iglesia, J. Phys Chem. B 2005, 109, 2155.

[6] G. A. Busca, S. Elmi, P.J. Forzatti, J. Phys. Chem. 1987, 91, 5236.

[7] C.R. Deltcheff, A. Aouissi, S. Launayb, M. Fournier, J. Mole. Catal. A: Chem. 1996, 33, 114.

[8] I. J. Shannon, T. Maschmeyer, R.D. Oldroyd, G. Sankar, J.M.Thomas, J. Chem. Soc. Fraday Trans. 1998, 94, 1495.

[9] S. Royer, X. Se ´cordel, M. Brandhorst, F. Dumeignil, S. Cristol, C. Dujardin, M. Capron, E. Payena, J.L. Dubois, Chem. Commun. 2008, 86, 57.

[10] H.Q Guo, D.B. Li, H.C Xiao, J.L. Zhang, W.H Li, Y.H. Sun, Korean J. Chem. Eng. 2009, 26, 902.

[11] Y.H. Zhang, I.J. Drake, D.N. Briggs, A.T. Bell, Synthesis of dimethyl carbonate and dimethoxy methane over Cu-ZSM-5, J. Catal. 2006, 244, 219.

[12] J.L. Gornay, X. Secordel, G. Tesquet, B.D. Menorval, S. Cristol, P. Fongarland, M. Capron, L. Duhamel, E. Payen, J.L. Dubois, F. Dumeignil, Green Chem. 2010, 12, 1722.

[13] Y. C. Fu, J. S. Shen, Chem. Commun. 2007, 72, 2121.

[14] Q. Sun, Y.C. Fu, J.W. Liu, A. Auroux, J.Y. Shen, Appl. Catal., A: Gen.2008, 334, 26.

[15] J.W. Liu, Y.C. Fu, Q. Sun, J.Y. Shen, Microporous Mesoporous Mater. 2008, 116, 614.

[16] S.Chen, S.P. Wang, X.B.Ma, J.L.Gong, Chem. Commun.2011, 47, 9345.

[17] F. Roozeboom, T. Fransen, P. Mars, P.J. Gellings, Z. Anorg. Allg. Chem.1979, 449, 25.

[18] G. Hausinger, H. Schmelz, H. Knijzinger, Appl. Catal.1988, 39, 267.

[19] M.P. Casaletto, L. Lisi, G. Mattogno, P. Patrono, F. Pinzari, G. Ruoppolo, Catal. Today 2004, 91, 271.

[20] B. G. Swierkoz, Appl. Catal. A: Gen.1997, 157, 263.

[21] R.Y. Saleh, I E. Wachs, S S Chan2, C C. Chersich, J. Catal. 1986, 98, 102

[22] M.A. Bañares, L.J. Alemanya, M.C. Jiménez, M.A. Larrubi, F. Delgado, M.L. Granados, A. Ma.Nez-Arias, J.M. Blasco, J.L. G. Fierro, J. Solid State Chem.1996, 124,69.

[23] P. Oliveira, M.L. Rojas-Cervantes, A.M. Ramos, I.M. Fonseca, A.M. Botelho do Rego, J. Vital, Catal. Today 2006, 118, 307 [24] M. A. Banares, L. J. Alemany, M. C Jime´nez,

M. A. Larrubia, F. Delgado, M. L. Granados, A. Martı´nez-Arias,J. M. Blasco, J. L. G. Fierro, J. solid state Chem.1996, 124, 69.

[25] H.Y Zhao, S. Bennici, J.X Cai, J.Y. Shen, A. Auroux, J. Catal. 2010, 274, 259.

[26] H.Y Zhao, S. Bennici, J.X Cai, J.Y. Shen, A. Auroux, Appl. Catal., A: Gene. 2010, 385, 224.

[27] J.P. Chen, R.T.Yang, J. Catal. 1993, 139, 277.

[28] J.P. Nogier, M. Delamar, Catal. Today 1994, 20, 109.

[29] V.I. Bukhtiyarov, Catal. Today 2000, 56, 403.

[30] M. Bensitel, O. Saur, J.C. Lavalley, Mater. Chem. Phys. 1988, 19, 147.

[31] L. Baraket, A. Ghorbel, P. Grange, Appl. Catal., B: Environ. 2007, 72, 37.

[32] J.B. Laizet, A.K. Søiland, J. Leglise, J.C. Duchet, Top. Catal. 2000, 10, 89.

[33] H.Q. Guo, D.B. Li, D. Jiang, W.H Li, Y.H. Sun, Catal.Today 2010, 158, 439.

[34] Z.H. Fan, H.Q.Guo, K.G. Fang, Y.H. Sun, RSC. Adv. 2015, 5, 24795

[35] K.V.R. Chary, G. Kishan , C. P. Kumar, U. V. Sagar, J.W. Niemantsverdriet, Appl. Catal., A: Gen.2003, 245, 303.

[36] A.S. Elmi, E.Tronconi, C. Cristiani, J. P. Gomez Martin, P. Forzatti. Ind. Eng. Chem. Res. 1989, 28, 387.

## Table and Figure Caption

**Table 1. The binding energies, surface and bulk composition of the catalysts and the distribution of sulfate**

**Table 2. The $NH_3$-TPD result and the calculated data.**

**Table 3. Influence of calcination temperature on DMM selectivity**

**Fig. 1. The XRD patterns of the catalysts**

**Fig. 2. The FT-IIR spectra of the catalysts**

**Fig. 3. XPS spectra of S2p for the catalysts**

**Fig. 4. The $H_2$-TPR-MS profiles of the catalysts: (a)VTS-673, (b) VTS -723，(c) VTS -773, (d) VTS -823 (e) VTS -873**

**Fig. 5. The TG profiles of the VTS catalyst**

**Fig. 6. The $NH_3$-TPD profiles of the catalysts**

**Fig. 7. Effect of calcination temperature on methanol conversion**

**Table 1. The binding energies, surface and bulk composition of the catalysts and the distribution of sulfate**

| Catalyst | $S_{BET}$ ($m^2.g^{-1}$) | Binding Energy (eV) | | | | Surface Composition (mol%)$^a$ | | | Bulk Composition (mol%)$^b$ | | | | No. of $SO_4^{2-}$ per unit area ($/nm^2$) | $S^a/S^b$ |
|---|---|---|---|---|---|---|---|---|---|---|---|---|---|---|
| | | O 1s | Ti $2p_{3/2}$ | V $2p_{3/2}$ | S2p | V | Ti | S | V | Ti | S | V/Ti$^b$ | | |
| VTS-673 | 64.4 | 529.7 (81.23%)<br>532.1(18.77%) | 458.2 | 516.4 | 168.7- | 25.89 | 65.26 | 8.85 | 20.48 | 73.2 | 6.32 | 0.28 | 6.95 | 1.40 |
| VTS-723 | 112.8 | 529.7 (85.11%)<br>532.0 (14.89%) | 458.4 | 517.1 | 168.9 | 27.22 | 66.14 | 6.64 | 20.96 | 73.69 | 5.35 | 0.28 | 3.38 | 1.24 |
| VTS-773 | 120.2 | 529.8 (87.87%)<br>532.0 (12.13%) | 458.3 | 517.1 | 168.9 | 27.68 | 66.54 | 5.78 | 22.31 | 73.1 | 4.59 | 0.31 | 2.74 | 1.26 |
| VTS-823 | 69.7 | 529.8 (90.36%)<br>531.9 (9.64%) | 458.4 | 517.2 | 169.4 | 28.54 | 66.93 | 4.53 | 21.29 | 74.59 | 4.12 | 0.29 | 4.20 | 1.16 |
| VTS-873 | 12.6 | 529.8 (95.36%)<br>531.9 (4.64%) | 458.4 | 517.2 | 169.5 | 30.03 | 67.32 | 2.65 | 22.16 | 75.32 | 2.52 | 0.30 | 14.54 | 1.05 |

**Table 2. The $NH_3$-TPD result and the calculated data.**

| Catalyst | No. of acidic sites (μmol/g) | No. of acidic sites per sulfate species |
|---|---|---|
| VTS-673 | 579.99 | 0.78 |
| VTS-723 | 745.49 | 1.18 |
| VTS-773 | 817.94 | 1.50 |
| VTS-823 | 384.80 | 0.79 |
| VTS-873 | 266.90 | 0.89 |

**Table 3. Influence of calcined temperature on DMM selectivity**

| Catalyst | Selectivity (%) | | | | |
|---|---|---|---|---|---|
| | FA | DME | MF | DMM | $CO_x$ |
| VTS-673 | 20.35 | 3.36 | 8.92 | 66.64 | 0.73 |
| VTS-723 | 3.23 | 0.94 | 5.16 | 90.33 | 0.34 |
| VTS-773 | 1.98 | 0.57 | 5.63 | 91.76 | 0.07 |
| VTS-823 | 7.26 | 1.10 | 8.28 | 83.21 | 0.15 |
| VTS-873 | 19.90 | 1.23 | 14.09 | 64.46 | 19.90 |

Reaction condition: $Ar/O_2/CH_3OH$=84.6/9.4/6.0 (v/v/v), 393 K, at about 45% methanol conversions

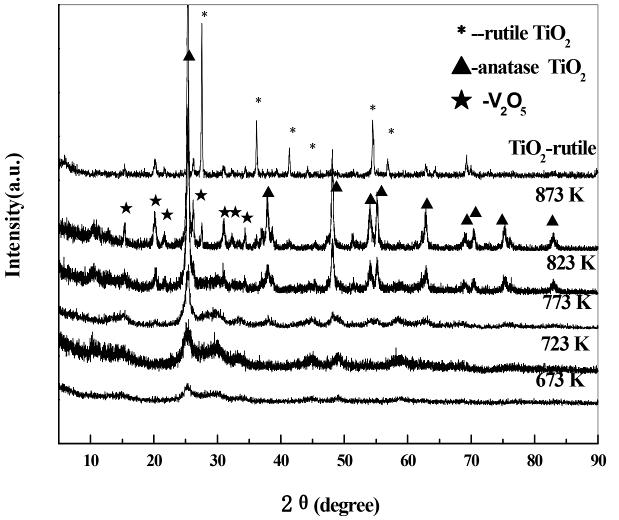

Fig. 1. The XRD patterns of the catalysts

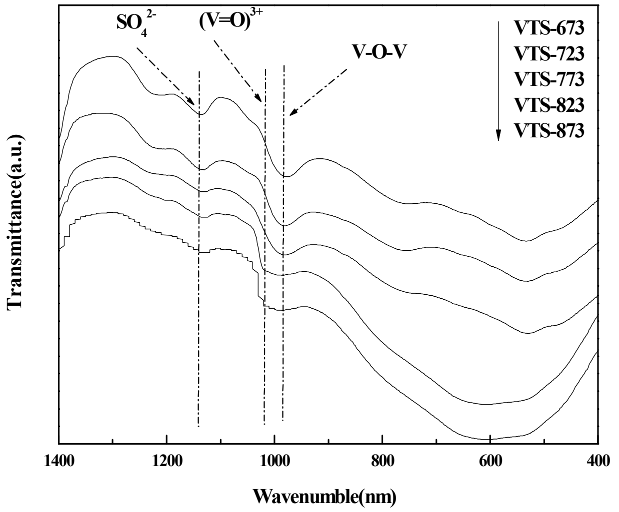

Fig. 2. The FT-IIR spectra of the catalysts

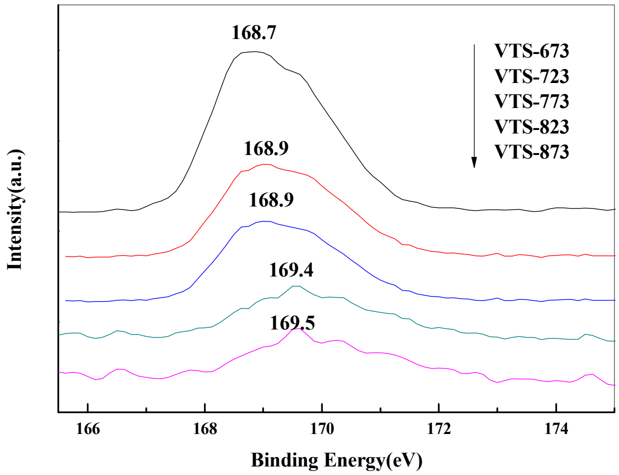

Fig. 3. XPS spectra of $S2p_{3/2}$ for the catalysts

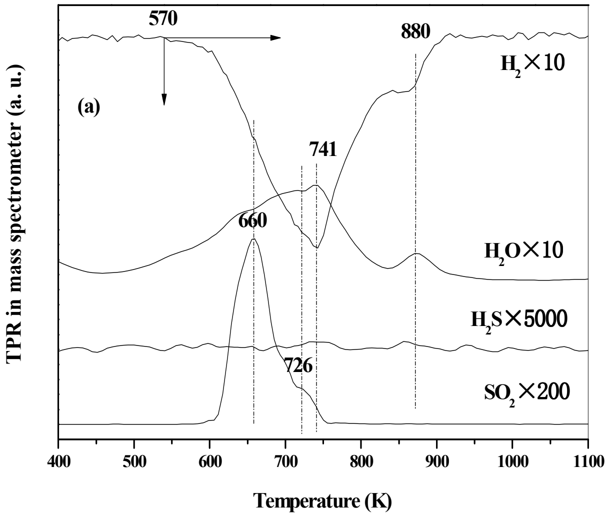

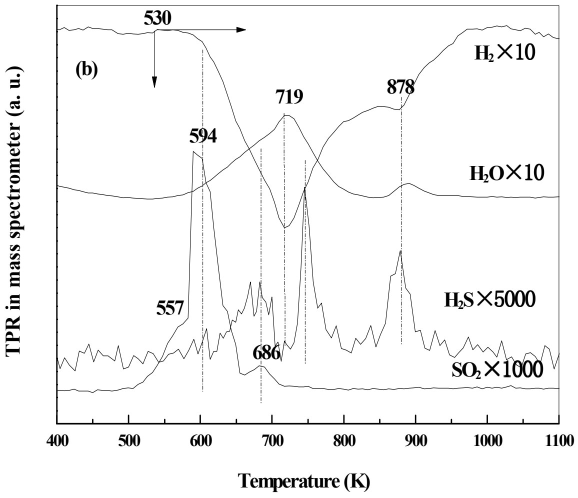
(b)
530
594
719
878
557
686
$H_2$×10
$H_2O$×10
$H_2S$×5000
$SO_2$×1000
TPR in mass spectrometer (a. u.)
Temperature (K)
400
500
600
700
800
900
1000
1100

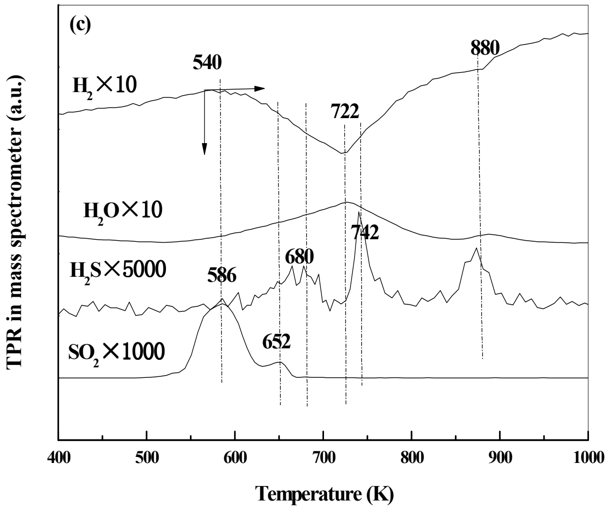
(c)
540
880
722
742
680
586
652
$H_2$×10
$H_2O$×10
$H_2S$×5000
$SO_2$×1000
TPR in mass spectrometer (a.u.)
Temperature (K)
400
500
600
700
800
900
1000

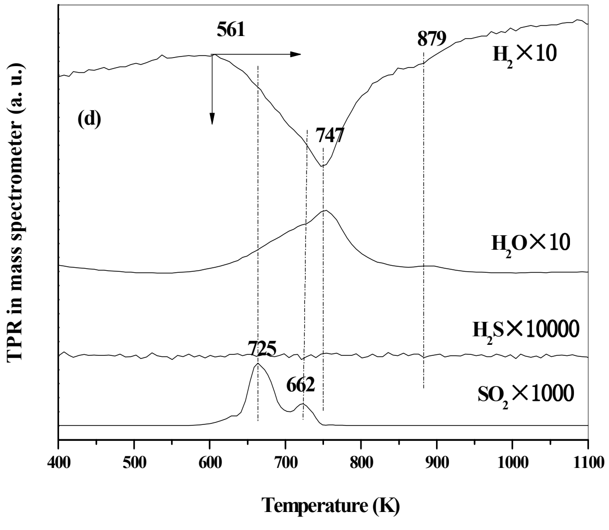
(d)
561
879
747
725
662
$H_2$×10
$H_2O$×10
$H_2S$×10000
$SO_2$×1000
TPR in mass spectrometer (a. u.)
Temperature (K)
400
500
600
700
800
900
1000
1100

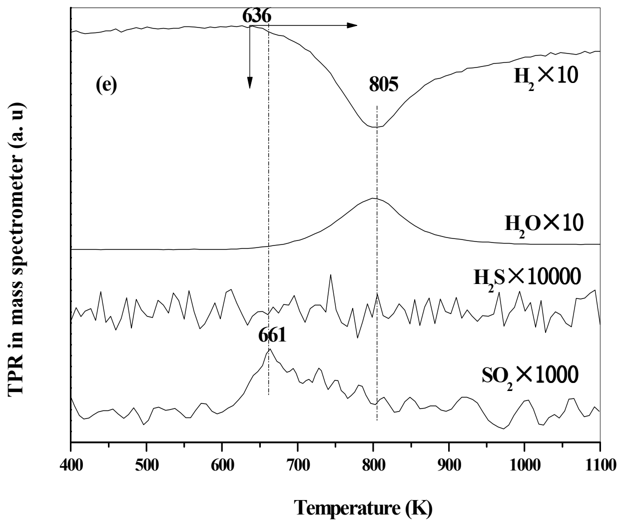

**Fig. 4. The $H_2$-TPR-MS profiles of the catalysts: (a) VTS-673, (b) VTS -723，(c) VTS -773, (d) VTS -823, (e) VTS -873**

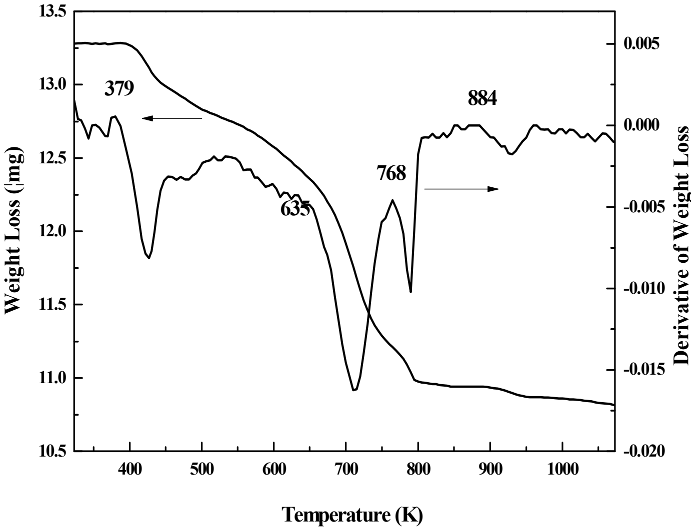

**Fig. 5. The TG profiles of the VTS catalyst**

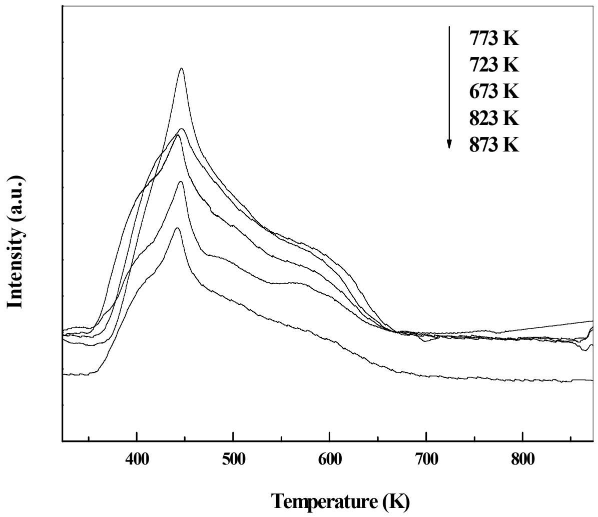

Fig. 6. The $NH_3$-TPD profiles of the catalysts

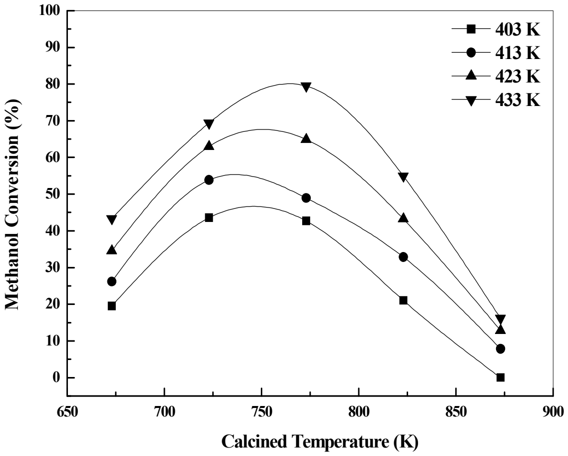

Fig. 7. Effect of calcination temperature on methanol conversion

# The One-step Oxidation of Methanol to Dimethoxymethane over Sulfated vanadia-titania Catalysts: Influence of Calcination Temperature

*Heqin Guo*[a], *Debao Li*[a], *Congbiao Chen*[a], *Litao Jia*[a], *Bo Hou*[a]*

[a] *State Key Laboratory of Coal Conversion, Institute of Coal Chemistry, Chinese Academy of Sciences, Taiyuan, 030001, China.*

**Corresponding author: Tel. /Fax: +86 351 4040087. E-mail addresses:*

houbo@sxicc.ac.cn,

The highest methanol conversion was obtained on catalysts calcined at 723 and 773 K

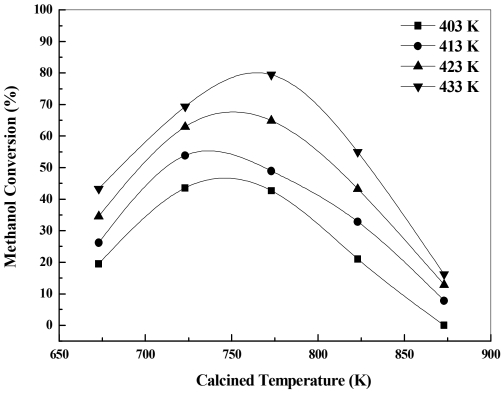

**Effect of calcination temperature on methanol conversion**